NASA TECHNICAL NOTE

NASA TN D-3251

EFFECTS OF A MAGNETIC FIELD ON THE CONDUCTION HEAT TRANSFER AT THE STAGNATION POINT OF A PARTIALLY IONIZED ARGON GAS

by James F. Schmidt

Lewis Research Center

Cleveland, Ohio

NATIONAL AERONAUTICS AND SPACE ADMINISTRATION • WASHINGTON, D. C. • FEBRUARY 1966

EFFECTS OF A MAGNETIC FIELD ON THE CONDUCTION HEAT TRANSFER AT THE STAGNATION POINT OF A PARTIALLY IONIZED ARGON GAS

By James F. Schmidt

Lewis Research Center
Cleveland, Ohio

NATIONAL AERONAUTICS AND SPACE ADMINISTRATION

For sale by the Clearinghouse for Federal Scientific and Technical Information
Springfield, Virginia 22151 – Price $2.00

EFFECTS OF A MAGNETIC FIELD ON THE CONDUCTION HEAT TRANSFER AT THE STAGNATION POINT OF A PARTIALLY IONIZED ARGON GAS

by James F. Schmidt

Lewis Research Center

SUMMARY

In a region of high electron-conduction heat flux (very high entry speeds) a magnetic field oriented parallel to the surface of the body can essentially eliminate the electron conduction heat flux and thereby reduce the total conduction heat transfer to the stagnation-point region. This conduction heat transfer is calculated for the following argon-gas stagnation-point flow conditions: pressures of 1.0, 0.1, 0.01, and 0.01 atmosphere at temperatures of 12 000°, 10 600°, 9500°, and 11 500° K, respectively. For the stagnation-point flow condition of 0.01 atmosphere and 11 500° K the maximum heat-transfer reduction (55 percent) is obtained for a magnetic-field strength of 12 000 gauss. The nonequilibrium boundary layer may have an even greater potential than the equilibrium boundary layer for a large heat-transfer reduction.

INTRODUCTION

Consideration of atomspheric entry at velocities of 45 000 feet per second and greater must include the effect of the ionization phenomena on the body heating. The presence of electrons in the gas surrounding a reentry body greatly increases the thermal conductivity of the gas and thereby the conduction heat flux to the body, depending upon the degree of ionization. Although the electrons have high mobility, which would increase the diffusion process of ion-electron pairs to the wall (where the large ionization energy can be released), the present report is concerned only with the conduction heat flux and thus gives a conservative estimate of the reduction possible by means of the properly oriented magnetic field.

Many analyses are available for determining the effect on the stagnation-point heat transfer produced by the interaction of a magnetic field with an electrically conducting fluid in a laminar boundary layer (e.g., refs. 1 to 3). These analyses conclude that only by the effect of the magnetic field on the inviscid flow (decreased velocity gradient) can the heat flux to a body be reduced. However, Chapman and Cowling (ref. 4) have shown that, in general, for a plasma, a magnetic field oriented perpendicular to the temperature gradient can reduce the heat flux to a surface independent of any magnetic-field effects on the inviscid flow. Reference 4 (p. 336) assumes that the gas is

composed of identically charged particles. In this report it is assumed that the results of reference 4 can be applied to the electron contribution to the conduction heat flux for a partially ionized gas in the stagnation-point region. In order to include the magnetic-field effects on the electron heat flux easily, the thermal conductivity and, thus, the conduction heat flux are separated into two parts, the neutral-atom and the electron thermal conductivity. Fay's mixture rule (ref. 5) for a partially ionized argon gas is used to calculate the conduction thermal conductivity of the neutral atoms and electrons. Although a partially ionized argon gas mixture is composed of ions as well as neutral atoms and electrons, the ion contribution to the conduction thermal conductivity is negligible until the gas becomes almost fully ionized (ref. 5). Argon (a simple monatomic gas) is selected for this study because its thermodynamic and transport properties have been explored experimentally as well as theoretically, even at very high temperatures.

A two-dimensional partially ionized flow around a circular cylinder with a constant, uniform magnetic field (parallel to the cylinder axis and thereby perpendicular to the stagnation-point heat flux) is analyzed at the stagnation point. This flow situation can easily be duplicated by shock-tube experiments. Since the problem of the inviscid flow around the cylinder, including Hall and ion slip effects, is presently not solved, the correct velocity gradient parameter at the edge of the boundary layer is not known. Therefore, solutions of the laminar-boundary-layer equations were obtained for several assumed values of the velocity-gradient parameter.

The numerical calculations were performed by Kenneth A. Pew and are described in appendix C.

ANALYSIS

Assumptions

Continuum flow in thermodynamic equilibrium is assumed for the two-dimensional boundary-layer flow. Additional assumptions are

(1) The induced magnetic field is negligible.

(2) The electrically conducting gas in the boundary layer maintains charge neutrality.

(3) The diffusion of the reacting argon gas species is neglected. (This could be a first-order effect at the highest temperatures considered.)

(4) There is negligible thermal radiation-energy absorption in the shock layer or boundary layer (ref. 6).

(5) Thermal diffusion is neglibible (ref. 7).

(6) Local similarity is assumed for solution of the boundary-layer equations.

Basic Equations

The general equations governing the flow of an electrically neutral conducting gas in a magnetic field are

Continuity:

$$\operatorname{div}(\rho\vec{V}) = 0 \tag{1}$$

Momentum:

$$\rho \frac{\vec{DV}}{Dt} = \vec{F} - \nabla P + \operatorname{div} \vec{\vec{\Psi}} \tag{2}$$

Energy:

$$\rho \frac{Dh}{Dt} + \operatorname{div} \vec{q} = \xi + \frac{DP}{Dt} + \vec{J} \cdot \vec{E}^* \tag{3}$$

where ρ and P are the density and pressure, respectively, at any point in the gas, $\vec{V}$ is the velocity vector, $\vec{F}$ is the Lorentz force vector, equal to $\vec{J} \times \vec{B}$, $\vec{B}$ is the magnetic-field vector, $\vec{\vec{\Psi}}$ is the shear stress tensor, h is the static enthalpy, and $\vec{q}$ is the heat-flux vector. (Symbols are defined in appendix A.) The effective electric field vector $\vec{E}^*$ from reference 8 is

$$\vec{E}^* = \vec{E} + \vec{V} \times \vec{B} + \frac{m_1 - m_2}{n(e_1 m_2 - e_2 m_1)} \nabla P - \frac{\rho P}{\rho_1 \rho_2} \frac{m_1 m_2}{e_1 m_2 - e_2 m_1} \nabla n_1 \tag{4}$$

where m is the particle mass, e is the particle charge, n is the number density, ∇n_1 is the ion concentration gradient, the subscript 2 indicates an electron, and the subscript 1 indicates an ion. The applied electric field vector $\vec{E}$ is assumed herein to be zero, and the velocity vector $\vec{V}$ is essentially zero for the stagnation flow region. The last two terms in equation (4) are diffusion effects due to the partial pressure gradient and the concentration gradient which are neglected in this analysis. Hence, the effective electric field vector $\vec{E}^*$ reduces to zero.

For zero ion slip, the current density vector $\vec{J}$, is given by reference 8 as

$$\vec{J} = \frac{\sigma\left[\vec{E}^* + \frac{\omega\tau_m}{B} \vec{B} \times \vec{E}^* + \frac{\omega^2\tau_m^2}{B^2} \vec{B}(\vec{B} \cdot \vec{E}^*)\right]}{1 + \omega^2\tau_m^2} \tag{5}$$

where σ is the scalar electrical conductivity of the gas and $\omega\tau_m$ is the Hall coefficient based on the momentum collision time (see appendix B). Since the effective electric field vector is zero in this study, the current density

vector (from eq. (5)) is also zero. The momentum and energy equations (2) and (3) in steady flow then reduce to

Momentum:

$$\rho(\vec{V} \cdot \nabla\vec{V}) = -\nabla P + \operatorname{div} \vec{\vec{\Psi}} \tag{6}$$

Energy:

$$\rho\vec{V} \cdot \nabla h = -\operatorname{div} \vec{q} + \xi + \vec{V} \cdot \nabla P \tag{7}$$

Scalar multiplication of the momentum equation (6) with $\vec{V}$ gives

$$\rho\vec{V} \cdot (\vec{V} \cdot \nabla\vec{V}) = -\vec{V} \cdot \nabla P + \vec{V} \cdot \operatorname{div} \vec{\vec{\Psi}} \tag{8}$$

Substituting for $\vec{V} \cdot \nabla P$ from equation (8) in equation (7) yields the energy equation as

$$\rho\vec{V} \cdot \nabla h = -\operatorname{div} \vec{q} + \vec{V} \cdot \operatorname{div} \vec{\vec{\Psi}} + \xi - \rho\vec{V} \cdot (\vec{V} \cdot \nabla\vec{V}) \tag{9}$$

If the usual boundary-layer assumptions (ref. 9) are made, $\operatorname{div} \vec{\vec{\Psi}}$, $\vec{V} \cdot \operatorname{div} \vec{\vec{\Psi}}$, and ξ are of the form

$$\operatorname{div} \vec{\vec{\Psi}} = \vec{j} \frac{\partial}{\partial y}\left(\mu \frac{\partial u}{\partial y}\right) \tag{10}$$

$$\vec{V} \cdot \operatorname{div} \vec{\vec{\Psi}} = u \frac{\partial}{\partial y}\left(\mu \frac{\partial u}{\partial y}\right) \tag{11}$$

$$\xi = \mu\left(\frac{\partial u}{\partial y}\right)^2 \tag{12}$$

where the velocity u is in the x-direction around the circular cylinder. These equations are valid if the viscous stress is assumed not to be a function of the magnetic field.

From appendix B, equation (B9), $\operatorname{div} \vec{q}$ is

$$\operatorname{div} \vec{q} = -\frac{\partial}{\partial y}\left(\frac{\lambda_A}{c_p} \frac{\partial h}{\partial y}\right) - \frac{\partial}{\partial y}\left(\frac{\lambda_E}{c_p(1 + \omega^2\tau^2)}\right) \frac{\partial h}{\partial y} \tag{13}$$

where c_p is the specific heat of the gas mixture at constant pressure, λ_A is the conduction thermal conductivity of the neutral atoms, λ_E is the conduction thermal conductivity of the electrons, and $\omega\tau$ is the Hall coefficient. From appendix B, equation (B14), $\omega\tau$ is

$$\omega\tau = \frac{15.20\ B}{T^{1/2}\ n_2} \frac{1}{\frac{S_{EA}}{\alpha} + \frac{1.331 \times 10^{-5}}{T^2}\left[3.943 + \log\left(\frac{T^3}{n_2}\right)^{1/2}\right]} \tag{14}$$

where T is the temperature in $^{\circ}K$, α is the degree of ionization, n_2 is the electron number density in electrons per cubic centimeter, B is the magnetic field in gauss, and S_{EA} is the electron - neutral-atom collision cross section and is assumed constant (3×10^{-16} cm^2) (see appendix B).

After equation (10) is substituted in equation (6), the momentum equation in the x-direction becomes

$$\rho u \frac{\partial u}{\partial x} + \rho v \frac{\partial u}{\partial y} = - \frac{dP_e}{dx} + \frac{\partial}{\partial y}\left(\frac{\mu \partial u}{\partial y}\right) \tag{15}$$

where

$$\frac{dP_e}{dx} = -\rho_e u_e \frac{du_e}{dx} \tag{16}$$

With the substitution of equations (11) to (13) in equation (9), the energy equation in terms of total enthalpy ($H = h + u^2/2$) in the stagnation region reduces to

$$\rho u \frac{\partial H}{\partial x} + \rho v \frac{\partial H}{\partial y} = \frac{\partial}{\partial y}\left(\frac{\lambda_A}{c_p}\frac{\partial H}{\partial y}\right) + \frac{\partial}{\partial y}\left(\frac{\lambda_E}{c_p(1 + \omega^2\tau^2)}\right)\frac{\partial H}{\partial y} \tag{17}$$

Finally, the following system of laminar-boundary-layer equations (for the stagnation region) is to be solved:

$$\rho u \frac{\partial u}{\partial x} + \rho v \frac{\partial u}{\partial y} = 0 \tag{18a}$$

$$\rho u \frac{\partial u}{\partial x} + \rho v \frac{\partial u}{\partial y} = \rho_e u_e \frac{du_e}{dx} + \frac{\partial}{\partial y}\left(\mu \frac{\partial u}{\partial y}\right) \tag{18b}$$

$$\rho u \frac{\partial H}{\partial x} + \rho v \frac{\partial H}{\partial y} = \frac{\partial}{\partial y}\left(\frac{\lambda_A}{c_p}\frac{\partial H}{\partial y}\right) + \frac{\partial}{\partial y}\left(\frac{\lambda_E}{c_p(1 + \omega^2\tau^2)}\frac{\partial H}{\partial y}\right) \tag{18c}$$

Transformed Equations

The following transformation equations (a slight modification of the transformation used by Lees (ref. 10)) for two-dimensional flow are used in the boundary-layer equations (18):

$$\eta = \frac{\rho_e (u_e)^{1/2}}{(\rho_w \mu_w)^{1/2}(2\bar{x})^{1/2}} \int_0^y \frac{\rho}{\rho_e}\, dy \tag{19a}$$

$$\bar{x} = x \tag{19b}$$

where the subscript e indicates conditions at the edge of the boundary layer and the subscript w indicates wall conditions. The derivatives transform as follows:

$$\frac{\partial}{\partial y} = \frac{\rho(u_e)^{1/2}}{(\rho_w u_w)^{1/2}(2\bar{x})^{1/2}} \frac{\partial}{\partial \eta} \tag{19c}$$

$$\frac{\partial}{\partial x} = \frac{\partial}{\partial \bar{x}} + \frac{\partial}{\partial \eta} \frac{\partial \eta}{\partial \bar{x}} \tag{19d}$$

and the stream function ψ, is defined so that

$$\rho u = \frac{\partial \psi}{\partial y} \tag{19e}$$

$$\rho v = - \frac{\partial \psi}{\partial x} \tag{19f}$$

Let

$$\psi = (\rho_w \mu_w)^{1/2}(u_e)^{1/2}(2\bar{x})^{1/2} f \tag{19g}$$

Then

$$f'(\eta) = \frac{u}{u_e} \tag{19h}$$

Also, let

$$g(\eta) = \frac{H(\eta)}{H_e} \tag{19i}$$

Applying the transformation equations (19) to the momentum and energy equations (18b) and (18c) and reducing give

Momentum:

$$(Cf'')' + ff'' + \beta\left[\frac{\rho_e}{\rho} - (f')^2 + \frac{ff''}{2}\right] = 0 \tag{20a}$$

Energy:

$$\left(\frac{D_A}{Pr_w} g' + \frac{D_E}{Pr_w} g'\right)' + fg'\left(1 + \frac{\beta}{2}\right) = 0 \tag{20b}$$

where Pr_w is the Prandtl number at the wall and β, the velocity gradient parameter, is

$$\beta = \frac{2\bar{x}}{u_e} \frac{du_e}{d\bar{x}} \tag{21}$$

The density ratio ρ_e/ρ is given by

$$\frac{\rho_e}{\rho} = \frac{1 + \alpha}{1 + \alpha_e} \frac{T}{T_e} \tag{22}$$

The density-viscosity ratio C referred to wall conditions ($T_w = 300^\circ$ K) is

$$C = \frac{\rho\mu}{\rho_w\mu_w} = \frac{T_w}{(1 + \alpha)T} \frac{\mu}{\mu_w} \tag{23}$$

where the viscosity μ is obtained from reference 11. The neutral-atom conduction heat-flux parameter D_A is

$$D_A = \frac{\rho}{\rho_w} \frac{c_{p,w}}{c_p} \frac{\lambda_A}{\lambda_w} = \frac{T_w}{(1 + \alpha)T} \frac{c_{p,w}}{c_p} \frac{\lambda_A}{\lambda_w} \tag{24}$$

Similarly, the electron-conduction heat-flux parameter D_E is

$$D_E = \frac{\frac{\rho}{\rho_w} \frac{c_{p,w}}{c_p} \frac{\lambda_E}{\lambda_w}}{1 + \omega^2\tau^2} \tag{25}$$

The neutral-atom thermal conductivity λ_A and the electron thermal conductivity λ_E (from ref. 5) are

$$\lambda_A = \frac{\lambda_A'}{1 + 1.44\ T^{0.16} \frac{\alpha}{1 - \alpha}} \tag{26}$$

$$\lambda_E = \frac{\lambda_E'}{1 + 0.78\times10^{-4} \frac{\lambda_E'}{\lambda_A'} \frac{1 - \alpha}{\alpha}} \tag{27}$$

where λ_A', the unionized neutral-atom thermal conductivity, is approximated by

$$\lambda_A' = 5.8\times10^{-7}\ T^{3/4} \tag{28}$$

and λ_E', the electron thermal conductivity for a fully ionized gas, is given by

$$\lambda_E' = \frac{4.4\times10^{-13}T^{5/2}}{\ln\left[\frac{1.24\times10^{4}T^{3/2}}{(n_2)^{1/2}}\right]} \tag{29}$$

The thermal conductivity at the wall λ_w is calculated from equation (26) with $\alpha = 0$ and $T = T_w$.

The following boundary conditions are applied to the transformed momentum and energy equations (20):

$$\left.\begin{aligned} f(w) = f'(w) &= 0 \\ f'(\eta) \to 1 \quad &\text{as} \quad \eta \to \infty \\ f''(\eta) \to 0 \quad &\text{as} \quad \eta \to \infty \\ g(w) &= g_w \\ g(\eta) \to 1 \quad &\text{as} \quad \eta \to \infty \\ g'(\eta) \to 0 \quad &\text{as} \quad \eta \to \infty \end{aligned}\right\} \tag{30}$$

Surface Heat Transfer

The conduction heat-transfer rate to a surface is

$$q = \lambda_w\left(\frac{\partial T}{\partial y}\right)_w \tag{31}$$

Substituting the transformation equations (19c) and (19i) and equation (21) into equation (31) and reducing yield the heat-transfer rate at the stagnation point:

$$q_s = \frac{(\rho_w\mu_w)^{1/2}}{Pr_w}\left(\frac{1}{\beta}\frac{du_e}{d\bar{x}}\right)^{1/2} H_e g_w' \tag{32}$$

The quantity $(1/\beta)(du_e/dx)$ is determined by the inviscid flow at the edge of the boundary layer. This inviscid flow is considered herein to be independent of the magnetic field, so that the ratio of heat-transfer rates with and without the magnetic field becomes

$$\frac{(q_s)_B}{(q_s)_{B=0}} = \frac{(g_w')_B}{(g_w')_{B=0}} \tag{33}$$

RESULTS AND DISCUSSION

Flow Property Variation Across Boundary Layer

The thermodynamic properties used in evaluating the flow coefficients in equations (20) were obtained from reference 11 for the following four stagnation-point flow conditions:

Pressure at edge of boundary layer, P_e, atm	Temperature at edge of boundary layer, T_e, ^oK
1.0	12 000
.1	10 600
.01	9 500
.01	11 500

The flow coefficients in equations (20) were calculated from equations (22) to (29) as a function of temperature for a given pressure but are plotted (figs. 1 and 2) as a function the enthalpy ratio g, which is one of the two dependent variables for the boundary-layer equations. Equations (20) were solved with an analog differential analyzer which gives results to four significant figures. The calculation method is described in appendix C. Equations (20) were also programed on a digital 7094 computer because the last stagnation-point flow condition was out of the range of accurate analog computer solutions.

The variation of the density-viscosity ratio C and the density ratio ρ_e/ρ (from eqs. (22) and (23)) as functions of the enthalpy ratio g, is shown in figure 1. The density-viscosity ratio falls to a very small value at the edge of the boundary layer (g = 1.0). Since this ratio is used only in the momentum equation in the present analysis, it has a negligible effect on the heat transfer.

The variation of the sum of the neutral-atom and electron heat-flux parameters (from eqs. (24) and (25)) as functions of the enthalpy ratio is shown in figure 2. The presence of the magnetic field is seen to reduce the total conduction heat flux through the boundary layer. The sum of the neutral-atom and electron conduction heat-flux parameters can also be expressed by the identity

$$D_A + D_E = D_A\left(1 + \frac{D_E}{D_A}\right)$$

The factor $1 + D_E/D_A$ shows more clearly the contribution of the electrons to the total heat flux (see fig. 3). Since

$$\frac{D_E}{D_A} = \frac{\frac{\lambda_E}{\lambda_A}}{1 + \omega^2\tau^2}$$

from equations (24) and (25), the effect of the magnetic field in reducing the electron portion of the heat flux is shown in figure 3. The degree of ionization α is also plotted in figure 3 to show that the electron heat flux is significant when the degree of ionization becomes appreciable.

The variation of the Hall coefficient $\omega\tau$ and the thermal-conductivity

ratio λ_E/λ_A in the boundary layer is shown in figure 4. At very small degrees of ionization the electron heat flux is negligible compared with the neutral-atom heat flux, and hence the magnetic field effect on the total heat flux is negligible even though the Hall coefficient becomes very large. For large degrees of ionization the thermal-conductivity ratio λ_E/λ_A increases and a greater potential effect of the magnetic field on heat transfer is possible. For comparable magnetic fields figure 4 shows a very large increase in the Hall coefficient as the pressure is reduced. This indicates that a significant viscous heat-flux reduction is possible for an equilibrium boundary layer with low pressures (P_e = 0.1 to 0.01 atm). A much larger heat-flux reduction appears possible for the low-pressure nonequilibrium boundary layer because in addition to large Hall coefficients the degree of ionization may also be larger and remain significant right up to the wall surface (ref. 12).

Solutions of Boundary-Layer Equations

Although the flow property variations in the boundary layer can provide qualitative effects on the heat transfer, the boundary-layer solutions for the highly nonlinear system of equations are required to predict quantitative results. Figure 5 presents these solutions in the form of the heat-transfer reduction ratio $(q_s)_B/(q_s)_{B=0}$ as a function of the applied magnetic field and stagnation flow condition. The solutions were calculated for values of the velocity-gradient parameter β ranging from 0 to 2.0. The single curve for each stagnation flow condition in figure 5 indicates that the ratio of heat transfer with and without a magnetic field is independent of β. However, the actual heat-transfer rate, with or without a magnetic field, depends significantly on the value of β (see fig. 6).

Figure 5 shows that the effect of the magnetic field on the heat-transfer ratio is accentuated at lower pressures and higher temperatures. For the two stagnation-point flow conditions at the same pressure (P_e = 0.01 atm) but different stagnation-point temperatures (9500° and 11 500° K), the degree of ionization is, respectively, 0.1177 and 0.6281. Therefore, the large difference in the heat-transfer reduction ratio between these two flow conditions is attributed to the effect of ionization. For each stagnation-point flow condition, the heat-transfer ratio levels off as the magnetic field is increased (see fig. 5). An explanation of this phenomenon is that, once the electron heat flux has been reduced to a negligible amount, the heat transfer is entirely due to the neutral atoms which are not affected by the magnetic field.

Lewis Research Center,
National Aeronautics and Space Administration,
Cleveland, Ohio, December 3, 1965.

APPENDIX A

SYMBOLS

A	$\frac{f\mathscr{P}_f\left(1+\frac{\beta}{2}\right)}{C}$
a,b,c	first, second, and third time division multiplier inputs
B	magnetic field
C	density-viscosity ratio (eq. (23))
$\mathscr{C}_2$	mean speed of electrons
c_p	specific heat of gas mixture at constant pressure
D_A	neutral-atom conduction heat-flux parameter (eq. (24))
D_E	electron conduction heat-flux parameter (eq. (25))
$\frac{D}{Dt}$	total substantial derivative, $\frac{\partial}{\partial t} + V \cdot \nabla$
E^*	effective electric field
e	particle charge
F	Lorentz force
f	integral of velocity distribution across boundary layer (eq. (19h))
g	total-enthalpy ratio, H/H_e
H	total enthalpy
h	static enthalpy
$\vec{i},\vec{j}$	unit vectors in x- and y-directions
$\vec{J}$	electric current density
k	Boltzman's constant
m	particle mass
n	number density of gas mixture
∇n_1	ion concentration gradient

P	static pressure
$\mathscr{P}_f$	defined by eq. (C4)
$\mathscr{P}_g$	defined by eq. (C3)
Pr	Prandtl number, $c_p\mu/\lambda$
$\vec{q}$	heat-flux or heat-transfer rate
R	$\beta[\rho_e/\rho - (f')^2]$
$\vec{r}$	position vector
S_{EA}	electron - neutral-atom collision cross section
S_{EI}	electron-ion collision cross section
T	static temperature
t	time
u	velocity parallel to cylinder surface
$\frac{du_e}{dx}$	velocity gradient at edge of boundary layer
$\vec{V}$	total flow velocity
v	velocity normal to cylinder surface
x	coordinate parallel to cylinder surface; $x = \bar{x}$
y	coordinate normal to cylinder surface
z	coordinate parallel to cylinder axis
α	degree of ionization
β	velocity-gradient parameter
ζ_e	constant, 1.865
η	similarity variable defined by eq. (19a)
λ_A	neutral-atom conduction thermal conductivity
λ_E	electron conduction thermal conductivity
λ_w	conduction thermal conductivity at wall
μ	coefficient of viscosity

ξ viscous dissipation function

ρ mass density

σ scalar electrical conductivity

τ electron energy collision time

τ_m electron momentum collision time

$\vec{\vec{\Psi}}$ shear stress

ψ stream function given by eq. (19g)

ω electron cyclotron frequency

Subscripts:

B with magnetic field

B=0 without magnetic field

e edge of boundary layer

s stagnation flow

w wall

1 ion

2 electron

Superscripts:

$\bar{}$ average

$\vec{}$ vector

$\vec{\vec{}}$ tensor

',","' derivatives with respect to η

APPENDIX B

CONDUCTION HEAT FLUX AND HALL COEFFICIENT

Conduction Heat Flux

Chapman and Cowling (ref. 4) have shown that a magnetic field (perpendicular to the conduction heat flux) will reduce the conduction heat flux for a gas composed of identically charged particles (electrons). This reduced electron heat flux (ref. 4) is

$$\vec{q}_2 = -\lambda_E \frac{\frac{\partial T}{\partial \vec{r}} - \frac{\omega\tau}{B} \vec{B} \times \frac{\partial T}{\partial \vec{r}}}{1 + \omega^2\tau^2} \tag{B1}$$

For two-dimensional flow with a constant magnetic field in the z-direction, the electron heat-flux equation (B1) becomes

$$\vec{q}_2 = - \frac{\lambda_E}{1 + \omega^2\tau^2} \left(\vec{i} \frac{\partial T}{\partial x} + \vec{j} \frac{\partial T}{\partial y} - \vec{j}\omega\tau \frac{\partial T}{\partial x} + \vec{i}\omega\tau \frac{\partial T}{\partial y} \right) \tag{B2}$$

The divergence of this electron conduction heat flux (eq. (B2)) gives

$$\operatorname{div} \vec{q}_2 = -\frac{\partial}{\partial x} \left(\frac{\lambda_E}{1 + \omega^2\tau^2} \frac{\partial T}{\partial x} \right) - \frac{\partial}{\partial y} \left(\frac{\lambda_E}{1 + \omega^2\tau^2} \frac{\partial T}{\partial y} \right)$$

$$- \frac{\partial}{\partial x} \left(\frac{\lambda_E \omega\tau}{1 + \omega^2\tau^2} \frac{\partial T}{\partial y} \right) + \frac{\partial}{\partial y} \left(\frac{\lambda_E \omega\tau}{1 + \omega^2\tau^2} \frac{\partial T}{\partial x} \right) \tag{B3}$$

Expanding the last two terms of equation (B3) gives

$$- \frac{\partial}{\partial x} \left(\frac{\lambda_E \omega\tau}{1 + \omega^2\tau^2} \frac{\partial T}{\partial y} \right) + \frac{\partial}{\partial y} \left(\frac{\lambda_E \omega\tau}{1 + \omega^2\tau^2} \frac{\partial T}{\partial x} \right) = - \frac{\lambda_E}{1 + \omega^2\tau^2} \omega\tau \frac{\partial}{\partial x} \left(\frac{\partial T}{\partial y} \right)$$

$$- \frac{\lambda_E}{1 + \omega^2\tau^2} \frac{\partial T}{\partial y} \frac{\partial(\omega\tau)}{\partial x} - \omega\tau \frac{\partial T}{\partial y} \frac{\partial}{\partial x} \left(\frac{\lambda_E}{1 + \omega^2\tau^2} \right) + \frac{\lambda_E}{1 + \omega^2\tau^2} \omega\tau \frac{\partial}{\partial y} \left(\frac{\partial T}{\partial x} \right)$$

$$+ \frac{\lambda_E}{1 + \omega^2\tau^2} \frac{\partial T}{\partial x} \frac{\partial(\omega\tau)}{\partial y} + \omega\tau \frac{\partial T}{\partial x} \frac{\partial}{\partial y} \left(\frac{\lambda_E}{1 + \omega^2\tau^2} \right) \tag{B4}$$

where

$$\frac{\partial(\omega\tau)}{\partial y} = \frac{\partial(\omega\tau)}{\partial T}\frac{\partial T}{\partial y} \tag{B5}$$

$$\frac{\partial(\omega\tau)}{\partial x} = \frac{\partial(\omega\tau)}{\partial T}\frac{\partial T}{\partial x}$$

$$\frac{\partial}{\partial y}\left(\frac{\lambda_E}{1+\omega^2\tau^2}\right) = \frac{\partial}{\partial T}\left(\frac{\lambda_E}{1+\omega^2\tau^2}\right)\frac{\partial T}{\partial y}$$

$$\frac{\partial}{\partial x}\left(\frac{\lambda_E}{1+\omega^2\tau^2}\right) = \frac{\partial}{\partial T}\left(\frac{\lambda_E}{1+\omega^2\tau^2}\right)\frac{\partial T}{\partial x}$$

Substituting equation (B5) into equation (B4) and reducing give

$$-\frac{\partial}{\partial x}\left(\frac{\lambda_E}{1+\omega^2\tau^2}\,\omega\tau\,\frac{\partial T}{\partial y}\right) + \frac{\partial}{\partial y}\left(\frac{\lambda_E}{1+\omega^2\tau^2}\,\omega\tau\,\frac{\partial T}{\partial x}\right) = 0 \tag{B6}$$

Therefore, equation (B3) reduces to

$$\operatorname{div}\vec{q}_2 = -\frac{\partial}{\partial x}\left(\frac{\lambda_E}{1+\omega^2\tau^2}\frac{\partial T}{\partial x}\right) - \frac{\partial}{\partial y}\left(\frac{\lambda_E}{1+\omega^2\tau^2}\frac{\partial T}{\partial y}\right) \tag{B7}$$

However, the first term in equation (B7) is very small compared with the second term. Hence, the divergence of the electron heat flux becomes

$$\operatorname{div}\vec{q}_2 = -\frac{\partial}{\partial y}\left(\frac{\lambda_E}{1+\omega^2\tau^2}\frac{\partial T}{\partial y}\right) \tag{B8}$$

For a partially ionized gas the atoms still conduct heat, but play a diminishing roll as the degree of ionization increases. Equation (B8) expresses the conduction heat flux of the electrons. Also, the magnetic field can only affect the charged particles (electrons) and not the neutral atoms. Therefore, the conduction heat flux (in terms of static enthalpy) is separated into two parts, the neutral-atom and the electron heat flux. The divergence of this conduction heat flux is

$$\operatorname{div}\vec{q} = -\frac{\partial}{\partial y}\left(\frac{\lambda_A}{c_p}\frac{\partial h}{\partial y}\right) - \frac{\partial}{\partial y}\left[\frac{\lambda_E}{c_p(1+\omega^2\tau^2)}\frac{\partial h}{\partial y}\right] \tag{B9}$$

Hall Coefficient

The Hall coefficient required to evaluate the electron heat flux can be expressed by the following equation:

$$\omega\tau = \frac{e_2 B}{m_2} \frac{\tau_m}{\zeta_e} \tag{B10}$$

where e_2 is the electron charge, m_2 is the electron mass, τ_m is the electron collision time based on the momentum transfer, and ζ_e is a constant (1.865) for a fully ionized gas (ref. 13) that reduces the electron collision time based on the momentum transfer to the electron collision time based on the energy transfer. For a fully ionized gas ζ_e is used in the partially ionized gas in the boundary layer for the following reasons:

(1) At very small degrees of ionization the electron heat flux is negligible compared with the neutral-atom heat flux, and hence the Hall effect on the heat flux is negligible (no matter how large the Hall coefficient becomes).

(2) At larger degrees of ionization (outer region of the boundary layer), the electron - neutral-atom collisions are negligible compared with the electron-ion collisions. Therefore, the partially ionized gas behaves like a fully ionized gas.

The electron collision time τ_m based on the momentum transfer can be approximated (from ref. 14) by

$$\tau_m = \frac{1}{n_2\left(\frac{S_{EA}}{\alpha} + S_{EI}\right)\bar{\mathscr{C}}_2} \tag{B11}$$

where $\bar{\mathscr{C}}_2$, the mean speed of the electrons, is

$$\bar{\mathscr{C}}_2 = \left(\frac{8kT}{\pi m_2}\right)^{1/2} \tag{B12}$$

Although the electron - neutral-atom collision cross section S_{EA} is not constant with temperature (see ref. 15), a constant value (3×10^{-16} cm^2) is used, for the same reasons as those for using the fully ionized gas value of the constant ζ_e. The electron-ion collision cross section is

$$S_{EI} = \frac{1.331\times10^{-5}}{T^2}\left[3.943 + \log\left(\frac{T^3}{n_2}\right)^{1/2}\right] \tag{B13}$$

Thus, the Hall coefficient becomes

$$\omega\tau = \frac{15.20\ B}{T^{1/2} n_2} \frac{1}{\frac{S_{EA}}{\alpha} + \frac{1.331\times10^{-5}}{T^2}\left[3.943 + \log\left(\frac{T^3}{n_2}\right)^{1/2}\right]} \tag{B14}$$

APPENDIX C

CALCULATION METHOD

by Kenneth A. Pew

The solution of equations (20) was obtained with the use of an EAI 16-31R analog computer. The computations were recorded with an EAI variplotter and a Brush recorder.

The first method attempted was the standard analog approach of solving for the highest order derivatives:

$$g'' = -g' \frac{D_A' + D_E' + Pr_w f\left(1 + \frac{\beta}{2}\right)}{D_A + D_E} \tag{C1}$$

$$f''' = - \frac{C' + f\left(1 + \frac{\beta}{2}\right) + \beta \frac{\rho_e}{\rho} - (f')^2}{C} \tag{C2}$$

The parameters ρ_e/ρ, C, D_A, and D_E were curved fitted as a function of g. The problem was then complicated by also requiring the evaluation of C', D_A', and D_E'. Various curve fit routines were used on an IBM 7094 digital computer to construct analytic expressions for C, D_A, and D_E. The analytic functions found were differentiated with respect to g and the derivatives set into the analog circuit on manual diode function generators. These derivatives were multiplied by g' to develop C', D_A', and D_E', and integrated to form C, D_A, and D_E. This process generated so much error in evaluating C', D_A', and D_E' that the results would be of little value.

This large error was avoided by using a transformation (see ref. 5) which eliminated the need for C', D_A', and D_E'. Let

$$\mathscr{P}_g = g'(D_A + D_E) \tag{C3}$$

$$\mathscr{P}_f = Cf'' \tag{C4}$$

The transformed equations then become

$$\mathscr{P}_g' = - \frac{Pr_w f \mathscr{P}_g \left(1 + \frac{\beta}{2}\right)}{D_A + D_E} \tag{C5}$$

$$\mathscr{P}_f' = - \frac{f\mathscr{P}_f \left(1 + \frac{\beta}{2}\right)}{C} - \beta\left[\frac{\rho_e}{\rho} - (f')^2\right] \tag{C6}$$

This made it possible simply to set the functions ρ_e/ρ, C, D_A, and D_E into the circuit on manual diode function generators (fig. 7). The circuit did require time scaling in order to slow the solution down by a factor of 5.

A trial solution was started by estimating the initial conditions g'_w and f''_w. The computer would then be operated and the results inspected. If the boundary conditions were not met, g'_w and/or f''_w would be altered. This procedure was repeated until the boundary conditions (eq. (21)) were satisfactorily met (±1 percent). Each computer operation required about 10 seconds. After the effects of the two initial conditions upon the system had become familiar, a solution could be obtained in approximately 5 minutes.

The greatest error involved in the solution was in the setting of the manual diode function generators. This error is estimated to be less than 2 percent.

REFERENCES

1. Neuringer, Joseph L.: Two-Dimensional Flow in the Vicinity of the Stagnation Point of an Incompressible, Viscous, Electrically Conducting Fluid in the Presence of a Magnetic Field. Republic Aviation Corp., June 12, 1957.

2. Meyer, Rudolph C.: On Reducing Aerodynamic Heat-Transfer Rates by Magnetohydrodynamic Techniques. J. Aerospace Sci. vol. 25, no. 9, Sept. 1958, pp. 561-566.

3. Bush, William B.: The Stagnation-Point Boundary Layer in the Presence of an Applied Magnetic Field. J. Aerospace Sci., vol. 28, no. 8, Aug. 1961, pp. 610-611.

4. Chapman, Sydney; and Cowling, T. C.: The Mathematical Theory of Nonuniform Gases. Second ed., Cambridge University Press, 1952 (reprinted 1963).

5. Fay, J. A.; and Kemp, N. H.: Theory of End Wall Heat Transfer in a Monatomic Gas, Including Ionization Effects. Rep. no. RR 166 (DDC no. AD-425461), Avco Research Laboratory, Mar. 1963.

6. Rutowski, R. W.; and Bershader, D.: Shock Tube Studies of Radiative Transport in an Argon Plasma. Phys. Fluids, vol. 7, no. 4, Apr. 1964, pp. 568-577.

7. Sherman, Martin P.: Calculation of Transport Properties of Mixtures of Helium and Partially-Ionized Argon. Rept. No. AEL 673 (DDC no. AD437625), Aeronautical Engineering Lab., Princeton Univ., Dec. 1963.

8. Wu, Ching-Sheng: A Generalized Ohm's Law of Plasma. Rept. No. JPL TR 32-23, Jet Propulsion Lab., California Institute of Technology, May 1960.

9. Schlichting, Hermann: Boundary Layer Theory. Fourth ed., McGraw-Hill Book Co., Inc., 1960.

10. Lees, Lester: Laminar Heat Transfer Over Blunt-Nosed Bodies at Hypersonic Flight Speeds. Jet Propulsion, vol. 26, no. 4, Apr. 1956, pp. 259-269.

11. Arave, R. J.; and Huseby, O. A.: Aerothermodynamic Properties of High Temperature Argon. Rept. No. D2-11238, Boeing Aircraft Co., 1962.

12. Camac, Morton; and Kemp, Nelson H.: A Multitemperature Boundary Layer. Paper No. 63-460, AIAA, Aug. 1963.

13. Burgers, J. M.: The Application of Transfer Equations to the Calculation of Diffusion, Heat Conduction, Viscosity, and Electric Conductivity. Part II. Tech. Note BN-124b (AFOSR - TN-58-427a), University of Maryland, May 1958.

14. Lin, Shao-Chi; Resler, E. L.; and Kantrowitz, Arthur: Electrical Conductivity of Highly Ionized Argon Produced by Shock Waves. J. Appl. Phys., vol. 26, no. 1, Jan. 1955, pp. 95-109.

15. Lyman, Fred A.; and Reshotko, Eli: Concerning the Need for Seeding in Nonequilibrium Magnetohydrodynamic Generator Channels. Paper 65 - WA/Ener-10, ASME, 1965.

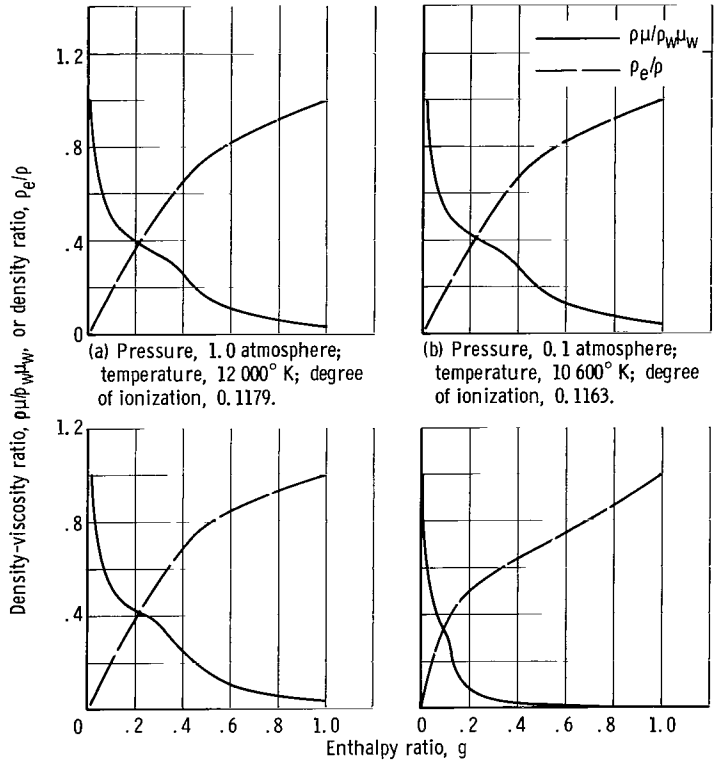

(a) Pressure, 1.0 atmosphere; temperature, 12 000° K; degree of ionization, 0.1179.

(b) Pressure, 0.1 atmosphere; temperature, 10 600° K; degree of ionization, 0.1163.

(c) Pressure 0.01 atmosphere; temperature, 9500° K; degree of ionization, 0.1177.

(d) Pressure, 0.01 atmosphere; temperature, 11 500° K; degree of ionization, 0.6281.

Figure 1. - Variation of density-viscosity ratio and density ratio with enthalpy ratio in boundary layer for various stagnation conditions.

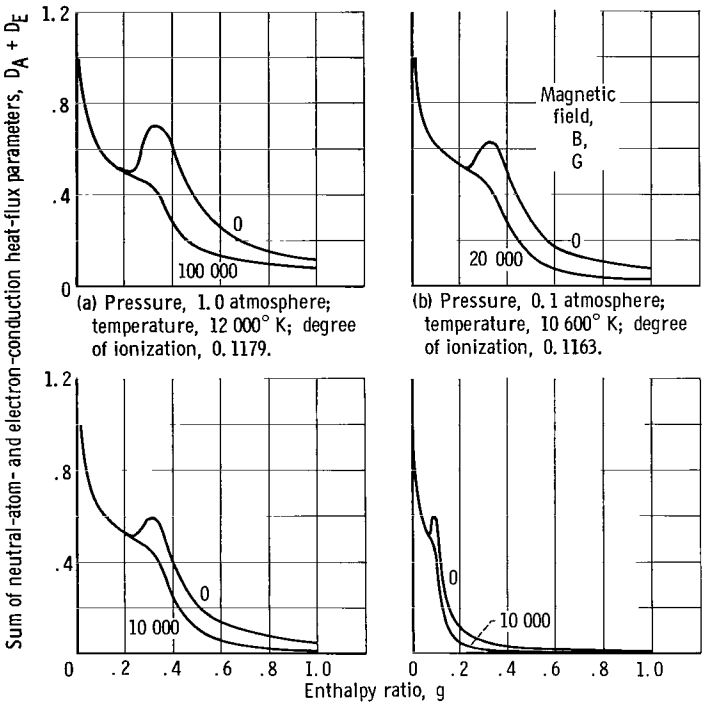

(a) Pressure, 1.0 atmosphere; temperature, 12 000° K; degree of ionization, 0.1179.

(b) Pressure, 0.1 atmosphere; temperature, 10 600° K; degree of ionization, 0.1163.

(c) Pressure, 0.01 atmosphere; temperature, 9500° K; degree of ionization, 0.1177.

(d) Pressure, 0.01 atmosphere; temperature, 11 500° K; degree of ionization, 0.6281.

Figure 2. - Variation of sum of neutral-atom- and electron-conduction heat-flux parameters with enthalpy ratio in boundary layer for various stagnation conditions.

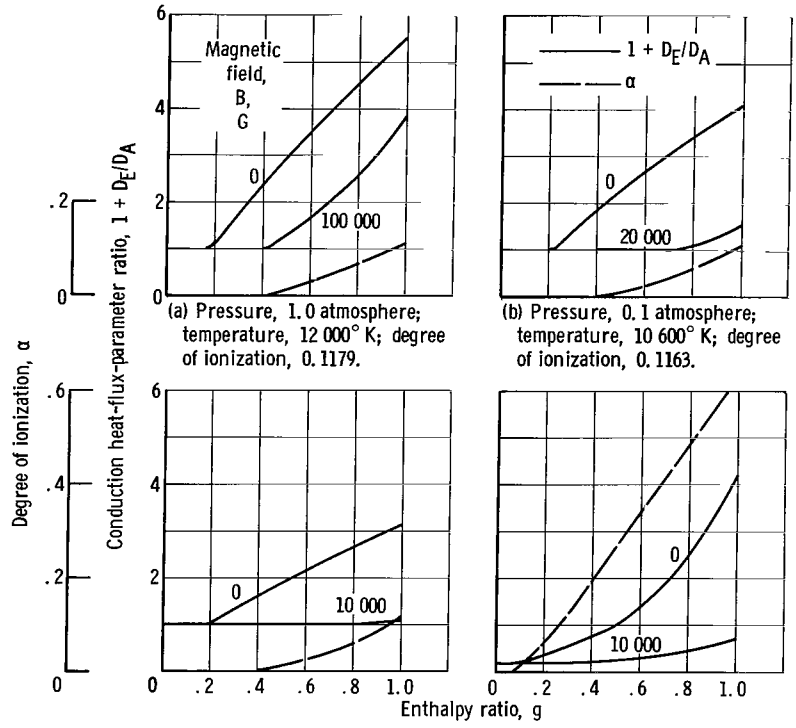

(a) Pressure, 1.0 atmosphere; temperature, 12 000° K; degree of ionization, 0.1179.

(b) Pressure, 0.1 atmosphere; temperature, 10 600° K; degree of ionization, 0.1163.

(c) Pressure, 0.01 atmosphere; temperature, 9500° K; degree of ionization, 0.1177.

(d) Pressure, 0.01 atmosphere; temperature, 11 500° K; degree of ionization, 0.6281.

Figure 3. - Variation of heat-flux-parameter ratio and degree of ionization with enthalpy ratio in boundary layer for various stagnation conditions.

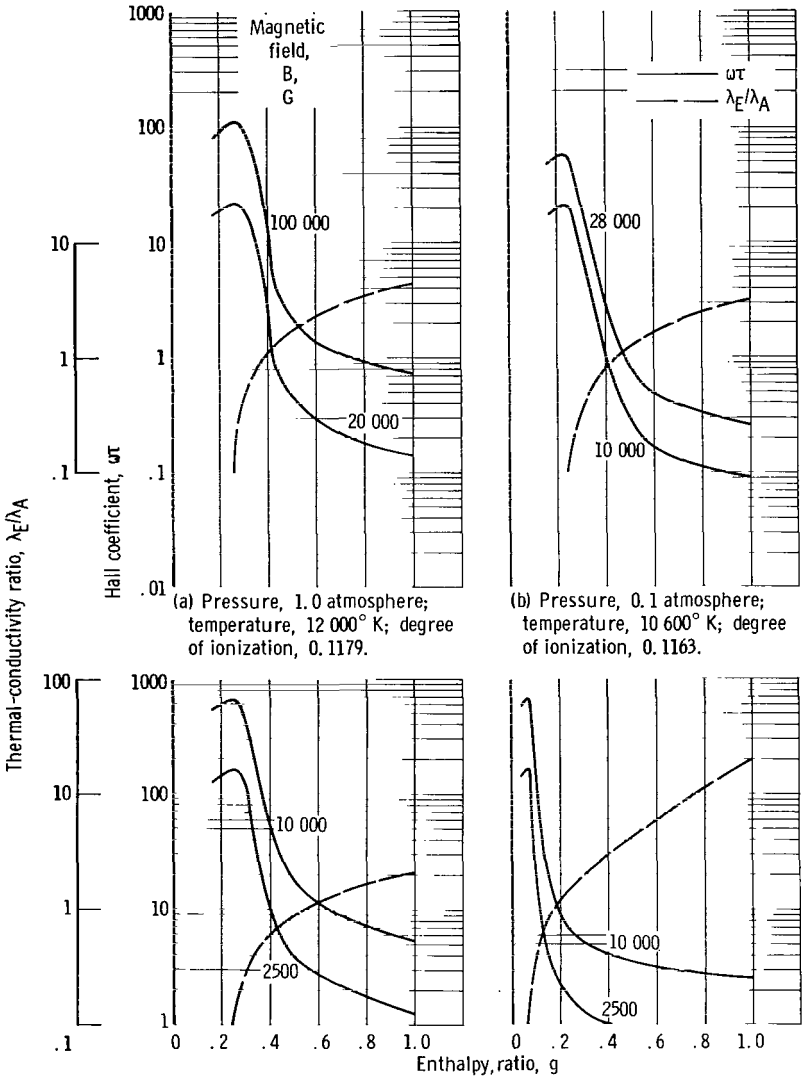

(a) Pressure, 1.0 atmosphere; temperature, 12 000° K; degree of ionization, 0.1179.

(b) Pressure, 0.1 atmosphere; temperature, 10 600° K; degree of ionization, 0.1163.

(c) Pressure, 0.01 atmosphere; temperature, 9500° K; degree of ionization, 0.1177.

(d) Pressure, 0.01 atmosphere; temperature, 11 500° K; degree of ionization, 0.6281.

Figure 4. - Variation of Hall coefficient and thermal-conductivity ratio with enthalpy ratio and magnetic-field strength for various stagnation conditions.

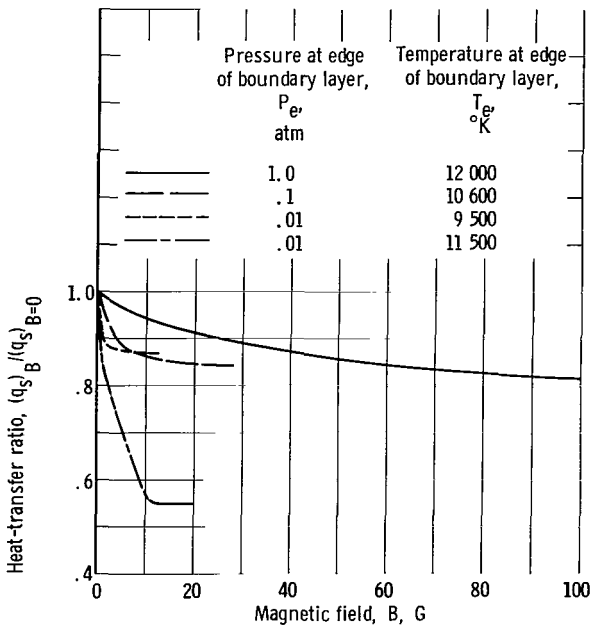

Figure 5. - Effect of magnetic field on heat-transfer ratio for equilibrium laminar boundary layer at stagnation point.

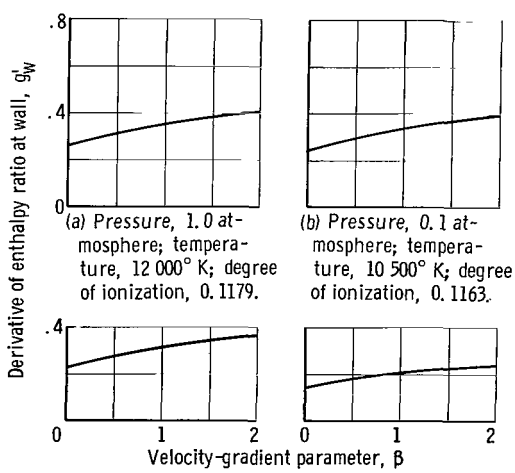

(a) Pressure, 1.0 atmosphere; temperature, 12 000° K; degree of ionization, 0.1179.

(b) Pressure, 0.1 atmosphere; temperature, 10 500° K; degree of ionization, 0.1163.

(c) Pressure, 0.01 atmosphere; temperature, 9500° K; degree of ionization, 0.1177.

(d) Pressure, 0.01 atmosphere; temperature, 11 500° K; degree of ionization, 0.6281.

Figure 6. - Effect of velocity-gradient parameter on heat transfer without magnetic field for various stagnation conditions.

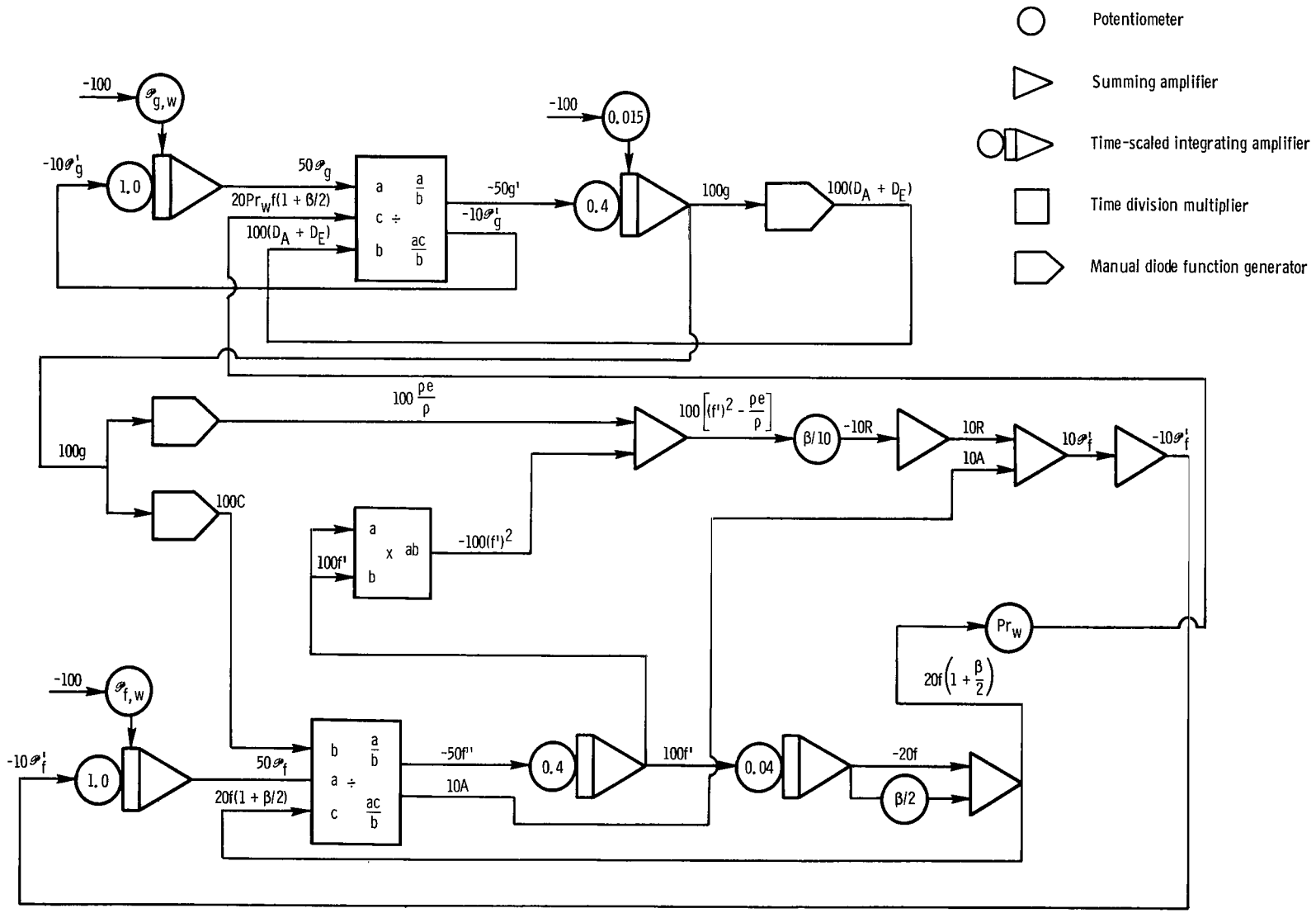

Figure 7. - Analog circuit diagram.

"The aeronautical and space activities of the United States shall be conducted so as to contribute . . . to the expansion of human knowledge of phenomena in the atmosphere and space. The Administration shall provide for the widest practicable and appropriate dissemination of information concerning its activities and the results thereof."

—NATIONAL AERONAUTICS AND SPACE ACT OF 1958

NASA SCIENTIFIC AND TECHNICAL PUBLICATIONS

TECHNICAL REPORTS: Scientific and technical information considered important, complete, and a lasting contribution to existing knowledge.

TECHNICAL NOTES: Information less broad in scope but nevertheless of importance as a contribution to existing knowledge.

TECHNICAL MEMORANDUMS: Information receiving limited distribution because of preliminary data, security classification, or other reasons.

CONTRACTOR REPORTS: Technical information generated in connection with a NASA contract or grant and released under NASA auspices.

TECHNICAL TRANSLATIONS: Information published in a foreign language considered to merit NASA distribution in English.

TECHNICAL REPRINTS: Information derived from NASA activities and initially published in the form of journal articles.

SPECIAL PUBLICATIONS: Information derived from or of value to NASA activities but not necessarily reporting the results of individual NASA-programmed scientific efforts. Publications include conference proceedings, monographs, data compilations, handbooks, sourcebooks, and special bibliographies.

Details on the availability of these publications may be obtained from:

SCIENTIFIC AND TECHNICAL INFORMATION DIVISION

NATIONAL AERONAUTICS AND SPACE ADMINISTRATION

Washington, D.C. 20546